

Nanoscale

Accepted Manuscript



This is an *Accepted Manuscript*, which has been through the Royal Society of Chemistry peer review process and has been accepted for publication.

Accepted Manuscripts are published online shortly after acceptance, before technical editing, formatting and proof reading. Using this free service, authors can make their results available to the community, in citable form, before we publish the edited article. We will replace this *Accepted Manuscript* with the edited and formatted *Advance Article* as soon as it is available.

You can find more information about *Accepted Manuscripts* in the [Information for Authors](#).

Please note that technical editing may introduce minor changes to the text and/or graphics, which may alter content. The journal's standard [Terms & Conditions](#) and the [Ethical guidelines](#) still apply. In no event shall the Royal Society of Chemistry be held responsible for any errors or omissions in this *Accepted Manuscript* or any consequences arising from the use of any information it contains.

Synthesis of N, F and S Co-Doped Graphene Quantum Dots

Sumana Kundu,^{a,b,c} Ram Manohar Yadav,^{c,d} T.N.Narayanan,^e Manjusha V Shelke,^{a,c,f} Robert Vajtai,^g P.M Ajayan,^{b,*} and Vijayamohanan K. Pillai^{a,b,f,*}

Received 00th January 20xx,
Accepted 00th January 20xx

DOI: 10.1039/x0xx00000x

www.rsc.org/

Graphene quantum dots (GQDs) are a promising category of materials with remarkable size dependent properties like tunable bandgap and photoluminescence along with the possibility of effective chemical functionalization. Doping of GQDs with hetero atoms is an interesting way of regulating their properties. Herein, we report a facile and scalable one-step synthesis of luminescent GQDs, substitutionally co-doped with N, F and S, of average size ~ 2 nm by a microwave treatment of multi-walled carbon nanotubes in a customized ionic liquid medium. This use of ionic liquid coupled with the use of a microwave technique enables not only an ultrafast process for the synthesis of co-doped GQDs, but also provides excellent photoluminescence quantum yield (70 %), perhaps due to the interaction of defect clusters and dopants.^{1,2}

With the advancement of nanoscience and technology many nanomaterials have been extensively studied for versatile applications utilizing their size and shape dependent properties. Quantum dots are one such class of nanomaterials well known for their variation of bandgap with size (band gap engineering) and consequently, several inorganic quantum dots like PbS, and CdSe have been used frequently in applications like sensors, field effect transistors, photodiodes and solar cells after achieving accurate size and shape control strategies.³ Despite their interesting properties, conventional quantum dots like PbS, and CdSe are extremely hazardous for processing and there are also innumerable challenges for disposal and recycling.³ Many of these limitations can be obviated by organic quantum dots such as graphene quantum dots (GQDs) to a great extent and hence many researchers consider

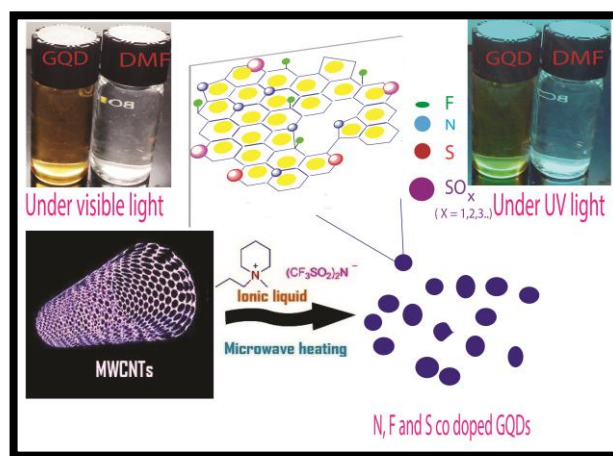


Figure 1. A schematic diagram indicating the formation of co-doped GQDs; inset shows a comparison of the same concentration of co-doped GQDs in DMF under visible light and UV light respectively (left: co-doped GQDs in DMF and right: DMF)

GQDs as a benign alternate to these conventional toxic quantum dots. Thus, GQDs, i.e. small fragments (usually up to 20 nm lateral size)⁴ of sp^2 hybridized 2D graphene layers with its π electrons confined in all three dimensions, unsurprisingly have grabbed the attention of many researchers due to its irresistible electronic⁵ properties, which could also be tuned by selective surface functionalization. Apart from tunable optical characteristics, several other exciting properties⁶⁻¹¹ like low cytotoxicity, low bandgap, tunable transport properties¹² with size and solubility control by surface functionalization have made this material a favorite for applications extending from energy storage to biomedical engineering.^{4,13-19}

Several synthetic methods are available for the size-controlled preparation of highly monodispersed GQDs such as hydrothermal cutting of graphene sheets (GSs), solvothermal cutting of GSs, nanolithography, electrochemical scissoring of GSs, chemical exfoliation, nanotomy (nanoscale-cutting) assisted exfoliation, ultrasonic shearing of GSs, stepwise organic synthesis of GQDs, precursor pyrolysis and surface catalyzed decomposition of fullerene.^{8,10,20-34} However, GQDs synthesized to date suffer from major drawbacks such as the involvement of multi-

^a Academy of Scientific & Innovative Research, Chennai, 600113, India.

^b CSIR-Central Electrochemical Research Institute (CSIR-CECRI), Karaikudi-630006, India.

^c Department of Materials Science and NanoEngineering, Rice University Houston, TX-77005, USA.

^d Department of Physics, VSSD College Kanpur-208002, India.

^e TIFR-Centre for Interdisciplinary Sciences, Tata Institute of Fundamental Research, Hyderabad-500 075, India.

^f CSIR-National Chemical Laboratory (CSIR-NCL), Pune-411008 MH, India.

E-mail: ajayan@rice.edu, vijay@cecri.res.in

Electronic Supplementary Information (ESI) available: [PLQY calculation, MWCNT synthetic details, TGA analysis and tabular format of GQD synthesis processes]. See DOI: 10.1039/x0xx00000x

COMMUNICATION

Journal Name

complex and laborious processes, relatively low yield, poor photoluminescence quantum yield (PLQY), and use of sophisticated and expensive equipment (especially for lithographic techniques). Moreover, many specific properties vary drastically from one synthetic route to another in an unpredictable manner; for example, the bottom-up approach gives bigger sized (60 nm) GQDs,³⁵ as compared to acidic oxidation, microwave, and thermal plasma processes which facilitate dots of smaller size distribution (2 ~ 4) nm.^{36,37,4} Furthermore, some of the hydrothermally prepared GQDs show pH-dependent Photoluminescence (PL),²² while similar electrochemically prepared GQDs show excitation dependent PL due to the fecundity of surface states.²⁰ Apart from these, couple of bulk production methods (such as that by Tour *et al.*) makes GQDs from coal³⁸ appreciable in terms of size control, and crystallinity, despite involving a substantial time. Similarly, thermal plasma jets³⁶ can produce GQDs in a large quantity although polydispersity is a major concern to be resolved. Microwave treatment of graphite in presence of KMnO_4 will also lead to bulk GQD production.³⁷ However, GQDs produced by the above methods show excitation dependent PL which deters their utilization for optoelectronic applications. Efforts are also being carried out to enhance the optical performance of GQDs either by doping or by surface passivation with organic ligands. Along with size reduction, doping with hetero atoms (such as B, N, S, and F) is also an effective method to tune the optical and electrical properties of GQDs. Doping of hetero atoms like nitrogen, sulfur, fluorine can open up a small bandgap in the electronic structure of GQDs and has shown their potential for some of the previously mentioned applications. Interestingly, Pristine GQDs always show a PLQY less than 33% and higher values are observed only after either functionalization or doping.³⁹ Among these dopants, N plays an important role in the electronic modification due to its comparable size with carbon (atomic radius: N - 56 pm, C - 70 pm). Theoretical studies have shown that carbon bearing the higher positive charge when adjacent to a N atom causes a positive shift in Fermi energy at the apex of the Brillouin zone of graphene.⁴⁰ In addition to this theoretical importance, recent experimental results show an improved electrocatalytic activity of N-doped graphene, akin to platinum and also a higher PLQY thus paving the way for a new generation of smart electrocatalysts, whose activity could be correlated with light emission.^{40,41} Recent studies have shown that apart from usual N or S doping, F doping in graphene can enhance the performance of Li ion batteries⁴² as well as F doping in carbon moiety improves ORR catalysis.⁴³ More studies are urgently needed in this direction and lastly there are very few studies on co-doping^{44,45} of hetero atoms in GQDs despite their potential significance.

Herein, we report such a facile, scalable, single-step synthesis of S, N, F co-doped GQDs by the microwave treatment of CNTs in an ionic liquid, namely {1-methyl-1-propylpiperidinium bis(trifluoromethylsulfonyl)imide}. The aim of using microwave heating is to accelerate the rate of reaction with a good yield compared to other conventional methods like hydrothermal treatment or conventional reduction of graphene oxide as illustrated in **Figure 1**. Moreover, the unique chemical structure of this ionic liquid facilitates efficient co-doping by N, S and F. Multiwalled CNTs (MWCNTs) were used as the precursor material for quantum dots and the ionic liquid acts

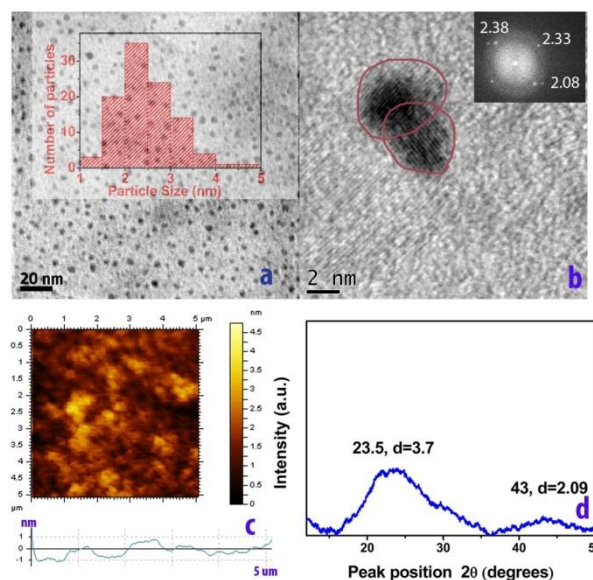


Figure 2. (a) TEM image of co-doped GQDs (in inset particle size distribution) (b) HRTEM image of co-doped GQDs (inset FFT pattern) (c) AFM image of co-doped GQDs (in inset height profile) and (d) Powder XRD pattern of co-doped GQDs

as a potent source for N, S as well as F. Using this strategy a very high yield (ca. 85%) could be obtained for GQDs along with a PLQY (70%) probably because of the enhanced kinetics, specific thermal effects and the defining features of the unique IL selected for this.

Figure 2 (a), shows a TEM image of the resultant co-doped GQDs exhibiting an average particle size of ~ 2 nm with a distribution of 1.5 to 4.5 nm range (shown in inset). **Figure 2** (b) is the corresponding HRTEM image and the inset shows the corresponding FFT (Fast Fourier Transform) pattern of the material. **Figure 2** (b) represents the clear lattice fringes with d spacing of 2.38, 2.33 and 2.08 respectively among which 2.08 matches with the powder XRD data shown in **Figure 2** (d). The d value 2.4 corresponds to the (100) crystal plane of graphite.²¹ The 2.38 could be due (100) pattern of graphene.⁴⁶ The d value of 2.08 i.e. (101) plane is very close to previously reported N, S doped GQDs (2.1).⁴⁶ Here a slight decrease in the d spacing in (100) plane (i.e. 2.4) to 2.38 is probably due to the presence of high N content (electronegativity- 3.04, atomic radius- 56 pm) in the in-plane graphene (electronegativity- 2.55, atomic radius - 70 pm) layer resulting in lattice contraction.

However, due to the bigger size of sulfur compared to carbon and also due to the difference in electronegativity between S and C (S - 2.58, C - 2.55), it is a daunting challenge to incorporate adequate amount of S in the graphene layer which results in relative low doping (~2.5%) of S as compared to N and F atoms. **Figure 2** (c) represents the atomic force microscopy (AFM) image of the GQDs (performed on a glass substrate) which shows a maximum height of 1 nm that corresponds to couple of layers (1-3) of graphene.

Raman spectroscopy is a very important tool to characterize the carbon samples. **Figure 3** (a) shows a typical Raman spectrum of GQDs with a prominent D band at 1367 cm^{-1} and a slightly less intense G band at 1585 cm^{-1} . The D band is related to the disorder produced due to size reduction and the G band is related to the in-plane vibration of the sp^2 carbon atoms. The observed I_D/I_G ratio of the synthesized GQDs is 1.04 which is a measure of defects which

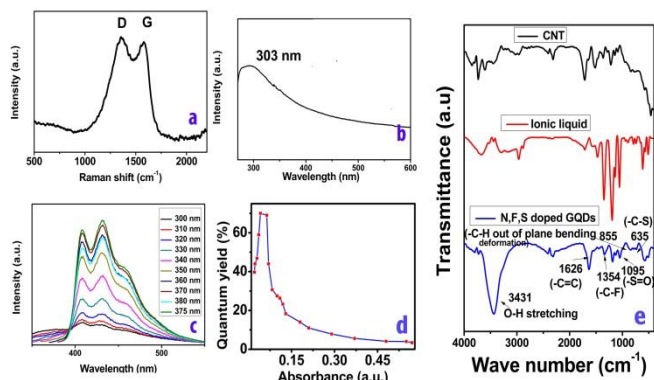


Figure 3. (a) Raman spectrum of co-doped GQDs (b) UV-VIS spectra of co-doped GQDs (c) PL spectra of co-doped GQDs (d) PLQY vs absorbance or concentration and (e) Comparative IR spectra of co-doped GQDs, IL and CNT

arise in GQDs not only due to doping but also due to reduction in size.²² The size reduction opens up more number of bare edges which are counted in Raman as defects. This is the reason that most of the GQDs usually show an I_D/I_G ratio more than 1.⁴⁷ Apart from this high I_D/I_G ratio, a broadened D and G peaks in Raman have been observed for this which are also seen in the previously reported samples of N doped GQDs.⁴⁸ **Figure 3** (b) shows the UV-Visible absorption spectrum of doped GQDs with a characteristic absorption peak at 303 nm. This spectrum matches well with that of the 320 nm peak for 9.6 nm hydrothermally²² prepared GQDs reported earlier, which is ascribed to n to n^* .

Figure 3 (c) shows a comparison of the PL emission spectra of GQDs as a function of the excitation wavelength from 325 nm to 380 nm (with a 10 nm interval) chosen to obtain the emission peak maxima. Interestingly, the spectra reveal an excitation-independent behavior of the GQDs as the peak positions of the emission maxima occur always at 409 nm and 435 nm respectively. The former peak arises probably due to singlet to singlet relaxation and the later one belongs to triplet to singlet transition (as the triplet excitons tend to have longer diffusion length).⁴⁹ Mueller *et al.*⁴⁹ have explored the shift in the peak position with different solvents and also the effect of solvent and size on singlet/triplet splitting. Similar kind of PL peaks have been observed in the GQDs prepared by other methods like thermal plasma jet.³⁶ Recent reports suggest the presence of intermediate surface states created upon functionalization with capping agent or organic molecule to be responsible for the excitation dependence⁵⁰ whereas excitation independent PL behavior probably mainly comes from the internal GQD structure (inter-band transition). In order to understand the intrinsic functional groups generated during the synthesis of the sample, IR (infrared) spectroscopy has been carried out accordingly on the GQD sample. The PLQY vs absorbance (which can be directly correlated to concentration term using Beer - Lambert's law; $A = \epsilon c l$, A = absorbance, ϵ = molar extinction coefficient, c = concentration l = path length) has been shown in **Figure 3** (d) to reveal a concentration or absorbance region corresponding to the maximum QY (70%) for a gaussian behavior, (0.042 to 0.07 absorbance region to get a high QY) whereas beyond this region QY diminishes and more details are provided in the supporting information (**Figure S2** and **Table S1**).

Figure 3 (e), shows a typical IR spectrum of the GQDs. Surprisingly, the IR spectrum does not show the commonly found C=O groups for oxidized GQDs. Rather, it shows a -C-F (1354 cm^{-1}), -S=O (1095 cm^{-1}), -C-S (635 cm^{-1}), -O-H / -N-H (3431 cm^{-1}) bond stretching vibrations which were further bolstered by the results of the XPS analysis. More specifically, these -S=O (1095 cm^{-1}), -C-S-C- (635 cm^{-1}) peaks resemble the IR spectra in the previously reported samples of both sulfur and nitrogen co-doped GQDs.⁴⁴ For a better understanding the IR spectra of CNT and IL have been provided along with the GQDs spectra. The spectrum of the doped GQDs is entirely different from the IL as well as CNT spectrum, indicating a change in the chemical environment in the doped GQDs. In order to assess the thermal stability and purity of the sample, thermogravimetric analysis (**Figure S3**) has been carried out in nitrogen atmosphere which shows a good stability upto 570°C . This indirectly suggests the absence of any unreacted IL since the observed $\sim 6\%$ weight loss at 352°C could be probably attributed to the decomposition of sulfone groups. More details are available in the supporting information (**Figure S3**).

Figure 4 (a) represents the XPS survey spectrum which confirms the presence of C, O, N, F and S with atomic concentration of 68.8%, 9.6%, 11.6%, 8.2% and 2.3% respectively. Deconvolution of the spectra gives six peaks for C 1s (**Fig 4** (b)) attributed to six bonding environments for carbon. A peak at 283.76 eV (a) represents the C-C, 284.5 eV (b) due to graphitic C=C, 284.8 eV (c) belongs to -C-N bonding, 286.1eV (d) is due to C-S, 286.6 eV (e) corresponds to C-O and 287.1 eV (f) due to C-F respectively. Similarly, three peaks for O 1s (**Figure 4** (c)) (a, b, c) have been obtained due to O-C, O-S, O-N bonding respectively. Figure 4 (d) shows four kind of nitrogen bonding starting from 398.16 eV (a) owing to pyridinic, 399.62 eV

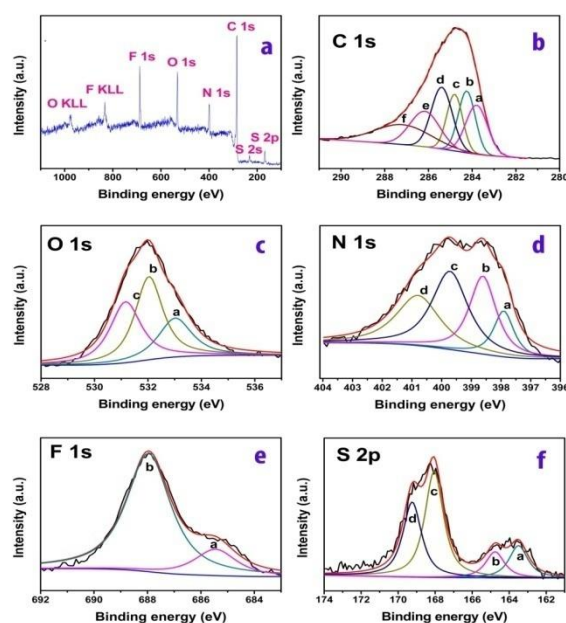


Figure 4. (a) XPS survey spectra of co-doped GQDs (b) XPS spectra of co-doped GQDs, C 1s (c) XPS spectra of co-doped GQDs, O 1s (d) XPS spectra of co-doped GQDs, N 1s (e) XPS spectra of co-doped GQDs, F 1s (f) XPS spectra of co-doped GQDs, S 2p

(b) due to pyrrolic, 400.73 eV (c) due to quaternary centre and 401.85 eV (d) for quaternary valley. Both pyridinic and pyrrolic

nitrogen are present in large amount compared to quaternary center and quaternary valley which may contribute in catalytic activity in ORR. **Figure 4** (e) depicts the F 1s spectra which contains two kind of bonding environment, 685.44 eV (a) owing to the semi ionic C-F bonding and 688 eV (b) due to covalent C-F bonding pattern. **Figure 4** (f) shows that S 2p spectrum has two peaks centered at 164.7 and 169.1 eV respectively indicating the presence of sulfur in two forms. Upon fitting of the 164.7 eV peak into two components at 163.8 (a) and 165.5 eV (b). These two peaks arise due to 2p_{3/2} and 2p_{1/2} positions of the **-C-S-C-** covalent bond of the thiophene like S respectively due to their spin-orbit couplings.⁵¹ The second peak consisting of 168.6(c) and 169.9 eV (d) corresponds to **-C-S(O)_x-C-**sulfone bridges.⁵¹ Here the more area in the peak of 168.6 and 169.9 eV indicates that S atom exists as sulfone bridges which matches with the -S=O stretch in IR at 1095 cm⁻¹. Li *et al.* also have observed this kind of sulfone bridges in their sulfur nitrogen co-doped GQDs.⁴⁴ Apart from these, table containing the yield, starting material, PLQY etc data have been provided in the supporting information (**Table S2**). The origin of enhanced luminescence could be explained by the dual effect of doping and size reduction. Thus the formation of GQDs with a good particle size distribution can be confirmed by TEM images which is also supported by all other complementary experimental data. Hetero atom doping in the GQDs lattice has been observed from the above XPS and IR data which also manifests from the high PLQY value of 70%. This high values are obtained only in the doped GQDs due to tailored electronic environment along with the size reduction in the graphene moiety. Recent report shows that these kind of co doping is promising in the area of visible light H₂ production and bio-imaging to overcome many material related challenges.⁴⁵

Conclusions

In summary, we have developed a rapid and easy technique to synthesize N, S and F co-doped GQDs in one step with a high yield of about 85% along with a higher QY of 70 % without using any tedious separation technique. As it is inclusively doped with three elements, an enhanced performance in the area of catalysis and energy application is expected. Apart from the catalysis field, most importantly the extremely high QY may lead to its application in the field of solar cells, light emitting diode. We hope to study and unravel the exciting properties of these doped GQDs in our future endeavors.

Experimental Section

Synthesis of N, S and F co-doped GQDs: 1 mg CNT was dispersed and sonicated in 1 ml of IL for 1 h and then kept inside the 1100 W microwave for 15 m. The resulting black powder was subsequently collected and dispersed in ethanol which turned yellowish brown (**Figure 1**. inset). This was filtered using a 0.2 μm PTFE membrane. The filtrate containing GQDs in ethanol was dried up under vacuum. After drying it can be redispersed in water and dialysed for 7-8 h.

Acknowledgements

We acknowledge IUSSTF joint center for the student exchange program on the project “3D engineered electrodes for

electrochemical energy storage” through grant number 22-2012/2013-14. RMY acknowledges the financial support from UGC, Govt. of India for the Raman Fellowship under Indo-21st Century knowledge Initiative. MVS acknowledge Indo-US Science and Technology Forum (IUSSTF), India for visiting fellowship. SK acknowledges CSIR for SRF fellowship. Authors thank Mr. A. Rathish Kumar and all other CIF staffs, CSIR-CECRI for their help rendered during the characterization of the samples. Authors thank **Prof. N. Ravishankar** (IISc Bangalore, India) and his **group (Ms. Dipanwita and Mr. Aakash)** members for the HRTEM imaging.

Notes and references

- 1 Y. Dong, H. Pang, H. Bin Yang, C. Guo, J. Shao, Y. Chi, C. M. and T. Yu, *Angew. Chemie - Int. Ed.*, 2013, **52**, 7800–7804.
- 2 Z. X. and Z. S. Dan Qu, Min Zheng, Peng Du, Yue Zhou, Ligong Zhang, Di Li, Huaqiao Tan, Zhao Zhao, *Nanoscale*, 2013, **5**, 12272–12277.
- 3 A. Valizadeh, H. Mikaeili, M. Samiei, S. M. Farkhani, Zarghami, M. Kouhi, A. Akbarzadeh and S. Davaran *Nanoscale Res. Lett.*, 2012, **7**, 480–494.
- 4 J. Shen, Y. Zhu, X. Yang and C. Li, *Chem. Commun. (Camb.)*, 2012, **48**, 3686–99.
- 5 M. A. Sk, A. Ananthanarayanan, L. Huang, K. H. Lim and F. Chen, *J. Mater. Chem. C*, 2014, **2**, 6954–6960.
- 6 K. a Ritter and J. W. Lyding, *Nat. Mater.*, 2009, **8**, 235–242.
- 7 C. O. Girit, J. C. Meyer, R. Erni, M. D. Rossell, C. Kisielowski, Yang, C.-H. Park, M. F. Crommie, M. L. Cohen, S. G. Louie and A. Zettl, *Science*, 2009, **323**, 1705–1708.
- 8 L. A. Ponomarenko, F. Schedin, M. I. Katsnelson, R. Yang, F. W. Hill, K. S. Novoselov and A. K. Geim, 2008, 356–358.
- 9 J. Güttinger, C. Stampfer, T. Frey, T. Ihn and K. Ensslin, *Phys. Status Solidi*, 2009, **246**, 2553–2557.
- 10 L.-J. Wang, G. Cao, T. Tu, H.-O. Li, C. Zhou, X.-J. Hao, Z. Su, G.-C. Guo, H.-W. Jiang and G.-P. Guo, *Appl. Phys. Lett.*, 2010, **97**, 262113–262114.
- 11 D. B. Shinde and V. K. Pillai, *Angew. Chem. Int. Ed. Engl*, 2013, **52**, 2482–2485.
- 12 J. Güttinger, F. Molitor, C. Stampfer, S. Schnez, A. Jacobsen, S. Dröscher, T. Ihn and K. Ensslin, *Rep. Prog. Phys.*, 2012, **75**, 1–25.
- 13 Z. Zhang, J. Zhang, N. Chen and L. Qu, *Energy Environ. Sci.*, 2012, **5**, 8869–8890.
- 14 S. Zhu, J. Zhang, S. Tang, C. Qiao, L. Wang, H. Wang, X. Liu, P. Li, Y. Li, W. Yu, X. Wang, H. Sun and B. Yang, *Adv. Funct. Mater.*, 2012, **22**, 4732–4740.
- 15 M.-L. Chen, Y.-J. He, X.-W. Chen and J.-H. Wang, *Bioconjug. Chem.*, 2013, **24**, 387–397.
- 16 J. Ju and W. Chen, *Biosens. Bioelectron.*, 2014, **58**, 219–225.
- 17 J. Ju and W. Chen, *Anal. Chem.*, 2015, **87**, 1903–1910.
- 18 J. Ju, R. Zhang, S. He and W. Chen, *RSC Adv.*, 2014, **4**, 52583–52589.
- 19 R. Zhang and W. Chen, *Biosens. Bioelectron.*, 2013, **55**, 83–90.
- 20 D. B. Shinde and V. K. Pillai, *Chemistry*, 2012, **18**, 12522–12528.
- 21 J. Peng, W. Gao, B. K. Gupta, Z. Liu, R. Romero-Aburto, L. Ge L. Song, L. B. Alemany, X. Zhan, G. Gao, S. A. Vithayathil, B. A. Kaiparettu, A. a Marti, T. Hayashi, J.-J. Zhu and P. M. Ajayari, *Nano Lett.*, 2012, **12**, 844–849.
- 22 D. Pan, J. Zhang, Z. Li and M. Wu, *Adv. Mater.*, 2010, **22**, 734–738.

- 23 S. Zhu, J. Zhang, C. Qiao, S. Tang, Y. Li, W. Yuan, B. Li, L. Tian, F. Liu, R. Hu, H. Gao, H. Wei, H. Zhang, H. Sun and B. Yang, *Chem. Commun. (Camb)*, 2011, **47**, 6858–6860.
- 24 D. Pan, L. Guo, J. Zhang, C. Xi, Q. Xue, H. Huang, J. Li, Z. Zhang, W. Yu, Z. Chen, Z. Li and M. Wu, *J. Mater. Chem.*, 2012, **22**, 3314–3318.
- 25 S. Zhu, J. Zhang, X. Liu, B. Li, X. Wang, S. Tang, Q. Meng, Y. Li, C. Shi, R. Hu and B. Yang, *RSC Adv.*, 2012, **2**, 2717–2720.
- 26 Y. Li, Y. Hu, Y. Zhao, G. Shi, L. Deng, Y. Hou and L. Qu, *Adv. Mater.*, 2011, **23**, 776–780.
- 27 M. Zhang, L. Bai, W. Shang, W. Xie, H. Ma, Y. Fu, D. Fang, H. Sun, L. Fan, M. Han, C. Liu and S. Yang, *J. Mater. Chem.*, 2012, **22**, 7461–7467.
- 28 R. Liu, D. Wu and X. Feng, *J. Am. Chem. Soc.*, 2011, **133**, 15221–15223.
- 29 Y. Zhu, G. Wang, H. Jiang, L. Chen and X. Zhang, *Chem. Commun. (Camb)*, 2014, **51**, 948–951.
- 30 N. Mohanty, D. Moore, Z. Xu, T. S. Sreepasad, A. Nagaraja, A. A. Rodriguez and V. Berry, *Nat. Commun.*, 2012, **3**, 1–8.
- 31 S. Zhuo, M. Shao and S.-T. Lee, *ACS Nano*, 2012, **6**, 1059–1064.
- 32 L. Tang, R. Ji, X. Cao, J. Lin, H. Jiang, X. Li and K. S. Teng, *ACS Nano*, 2012, 5102–5110.
- 33 J. Lu, P. S. E. Yeo, C. K. Gan, P. Wu and K. P. Loh, *Nat. Nanotechnol.*, 2011, **6**, 247–252.
- 34 J.-J. Li, Linling; Wu, Guohai; Peng, Juan; Zhao, Jianwei; Zhu, *Nanoscale*, 2013, **5**, 4015–4039.
- 35 X. Yan, X. Cui and L.-S. Li, *J. Am. Chem. Soc.*, 2010, **132**, 5944–5955.
- 36 J. Kim and J. S. Suh, *ACS Nano*, 2014, **8**, 4190–4196.
- 37 Y. Shin, J. Lee, J. Yang, J. Park, K. Lee, S. Kim, Y. Park and H. Lee, *Small*, 2014, **10**, 866–870.
- 38 R. Ye, C. Xiang, J. Lin, Z. Peng, K. Huang, Z. Yan, N. P. Cook, E. L. G. Samuel, C.-C. Hwang, G. Ruan, G. Ceriotti, A.-R. O. Raji, A. a Martí and J. M. Tour, *Nat. Commun.*, 2013, **4**, 1–6.
- 39 L. Li, G. Wu, G. Yang, J. Peng, J. Zhao and J.-J. Zhu, *Nanoscale*, 2013, **5**, 4015–4039.
- 40 D. Geng, S. Yang, Y. Zhang, J. Yang, J. Liu, R. Li, T.-K. Sham, X. Sun, S. Ye and S. Knights, *Appl. Surf. Sci.*, 2011, **257**, 9193–9198.
- 41 D. Qu, M. Zheng, L. Zhang, H. Zhao, Z. Xie, X. Jing, R. E. Haddad, H. Fan and Z. Sun, *Sci. Rep.*, 2014, **4**, 1–9.
- 42 D. Damien, P. M. Sudeep, T. N. Narayanan, M. R. Anantharaman, P. M. Ajayan and M. M. Shaijumon, *RSC Adv.*, 2013, **3**, 25702.
- 43 X. Sun, Y. Zhang, P. Song, J. Pan, L. Zhuang, W. Xu and W. Xing, *ACS Catal.*, 2013, **2000**, 1726–1729.
- 44 B.-X. Zhang, H. Gao and X.-L. Li, *New J. Chem.*, 2014, **38**, 4615–4621.
- 45 D. Qu, Z. Sun, M. Zheng, J. Li, Y. Zhang and G. Zhang, *Adv. Opt. Mater.*, 2015, **3**, 360–367.
- 46 Z. Q. Li, C. J. Lu, Z. P. Xia, Y. Zhou and Z. Luo, *Carbon N. Y.*, 2007, **45**, 1686–1695.
- 47 M. Bacon, S. J. Bradley and T. Nann, *Part. Part. Syst. Character.*, 2014, **31**, 415–428.
- 48 Y. Li, Y. Zhao, H. Cheng, Y. Hu, G. Shi, L. Dai and L. Qu, *J. Am. Chem. Soc.*, 2012, **134**, 15–18.
- 49 M. L. Mueller, X. Yan, J. a McGuire and L. Li, *Nano Lett.*, 2010, **10**, 2679–2682.
- 50 G. S. Kumar, R. Roy, D. Sen, U. K. Ghorai, R. Thapa, N. Mazumder, S. Saha and K. K. Chattopadhyay, *Nanoscale*, 2014, **6**, 3384–3391.
- 51 S. Li, Y. Li, J. Cao, J. Zhu, L. Fan and X. Li, *Anal. Chem.*, 2014, **86**, 10201–10207.